Crack growth stability analysis with respect to boundary disturbance

Hao Chen[1,*]

[1] Key Laboratory of Earthquake Engineering and Engineering Vibration,
Institute of Engineering Mechanics, CEA, Sanhe, 065201, China
* Corresponding author: chenhao@iem.ac.cn

Abstract Fracture analysis is a high non-linear problem and affected by uncertainties. Because of the limitation of observing technology, accuracy boundary condition can hardly be obtained. Normally, a stochastic model can be used. The difference between reality and numerical model is deemed as disturbance. This paper presents a three-dimension dynamic stability analysis of crack growth under disturbance in boundary condition by using particle discretization scheme finite element method.

The model is a thin epoxy plate with two anti-symmetric notches located in the middle, under uni-axial tensile in longitudinal direction. Two types of disturbance are considered: (i), the disturbance is added to the initial cracks' configuration. The disturbance is modeled by adjusting the position, size and shape of the notches. It shows that changes of the notches' size and position have significant influence on crack growth in the investigated cases; (ii), the disturbance is applied to the displacement boundary condition, which is far from initial cracks. The variability of crack paths of different model sizes under the same disturbance is estimated. The results of the numerical experiment indicate that as the model size increases, the influence of the disturbance becomes weaker. The Saint-Venant principle still holds in the studied crack growth problem.

Keywords Three dimensional dynamic crack growth, particle discretization scheme, finite element method, boundary disturbance, stability analysis

1. Introduction

Fracture analysis is a hot topic in solid mechanics [1]. Both experiments [2] and numerical methods have been developed to investigate the fracture behavior. The physical experiment is a reliable way. However, it costs a lot of resources to conduct. As the accumulation of experimental data increases, the fracture mechanics of more and more materials can be studied by using numerical method, for its convenience and resources saving. In order to increase the reliability of simulation results, a numerical model needs to be built as accurately as possible. However, the current observation equipments and technology have their limitation. Therefore, differences between reality and numerical model exist. Normally, stochastic model can be proposed, and the average value with variances can be used in numerical simulation. The difference between reality and numerical setting is deemed as disturbance in this paper. Since the crack drastically changes the stiffness matrix and strain energy, the dynamic crack propagation becomes a high non-linear problem. Hence, the results may be affected by these uncertainties. In mathematical view point, instability means that when a small perturbation is added to a system, the results will drastically change.

This paper focuses on studying the effect of the boundary condition disturbance on an elastic dynamic fracture problem. The well known Saint-Venant principle tells that, as the distance between the target and disturbance source increases, the effect of the disturbance decreases. Meanwhile, Oguni et al. [3] states that for dynamic fracture stability analysis, the uncertainties can be deemed as disturbance added to the stiffness matrix. As time increases, the effect may be increased or maintained according to system property. Based on these two theories, for boundary disturbance problems, it can be inferred that the effect of disturbance in boundary condition fades as the distance from area of interest increases, and heightens or maintains as time increases. However, since the property of dynamic fracture problem is nonlinear, the effects need to be quantificationally estimated.

Both experiment and numerical simulation can be used to study the effect of boundary disturbance. However, there is an advantage to examine the boundary disturbance effect by using numerical methods. At least two samples are needed to conduct this comparison study. The ideal situation is that all the settings are the same except that a specified disturbance is added in one of the samples' boundary condition. However, in reality, the variability of samples is hard to control, and the designed disturbance in boundary condition cannot be accurately applied. These uncertainties may lead to side effects on this comparison study. While in the numerical analysis, it is much easier to define identical models and add the specified disturbances exactly.

This paper studies the effect of two kinds of boundary disturbances, say, the near and far field disturbances. Here, the adjective, "near" and "far" are used to describe the distance between the boundary with disturbance and the region where crack grows. The target is a thin epoxy resin plate with two anti-symmetric notches located in the middle, subjected to uni-axial tensile in longitudinal direction. The near field disturbance is modelled by adjusting the position, size and shape of the notches. The far field disturbance is modelled by adding disturbance to the displacement boundary condition, which is far from the notches. Several kinds of disturbances are adopted. In order to study the Saint-Venant principle in the fracture problem, the crack paths of different model sizes under the same disturbance are compared.

For numerical simulation of fracture problems, various kinds of numerical methods have been proposed, such as E-FEM, X-FEM [4], discontinuous Galerkin method [5] and meshfree methods [6]. Besides these methods, the newly developed method, called particle discretization scheme finite element method (PDS-FEM) is another candidate [7,8] to calculate three dimensional dynamic crack propagation, for its numerical efficiency and capability of calculating bifurcation, which is important for brittle materials, such as epoxy resin, rock and concrete.

The content of the present paper is as follows: section 2 briefly introduces the characteristics of the adopted numerical method, PDS-FEM. Section 3 and 4 are devoted to study the effect of near and far field disturbances, respectively. Concluding remarks are pointed out in section 5.

2. PDS-FEM

The key idea of PDS-FEM is the discretization scheme. PDS or particle discretization scheme is a scheme which uses two sets of non-overlapping characteristic functions to discretize a function and its derivative. One set is made for Voronoi tessellation, and characteristic functions of this tessellation used to discretize a function. The other set is made for Delaunay tessellation, and characteristic functions of this tessellation are used to discretize function derivatives.

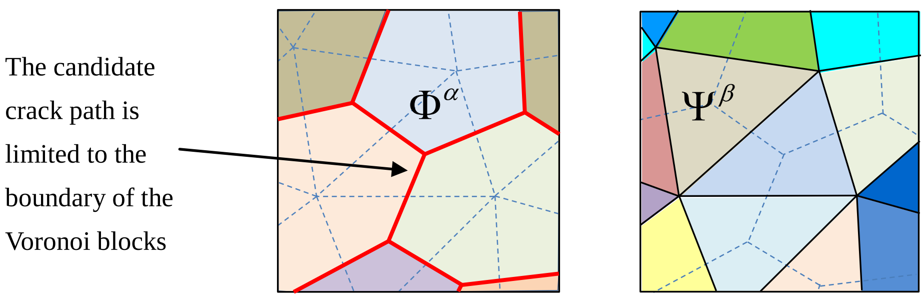

Voronoi tessellation Delaunay tessellation

Figure 1. Two dimension decomposition by using particle discretization scheme

Displacement is discretized by the Voronoi, while strain and stress is discretized by Delaunay. As you can see in Fig. 1, discretized functions are discontinuous everywhere. So, it is easy to model a crack, which is the discontinuity in a function of displacement. The candidate crack paths are limited to the boundary of the Voronoi blocks. For three dimensions decomposition, we can use ordinary tetrahedral mesh instead of triangular mesh as the Delaunay tessellation, and then for each tetrahedral vertex, the Voronoi block containing the vertex is determined by connecting all the centroids of tetrahedrons containing the vertex.

For dynamic analysis, a variation integrator called bilateral symplectic algorithm [9] is adopted as a robust algorithm of the time integration in PDS-FEM [8]. This algorithm is robust for stiffness matrix changes due to crack propagation. Meanwhile it is symplectic, which indicates that the momentum and energy are conserved during the numerical integration.

3. Near field disturbance modeling and simulation

Nowadays, the underground velocity structure and the hypocenter still can hardly be modeled accurately [10-12], let alone the detail fault configuration. According to previous researches, one of the best published results of underground velocity structure modeling with the help of the densest distribution of observation stations in Japan still has more than 10% error [13]. In order to carry out earthquake simulation, the configuration of the fault is always estimated with some variances. The effect of the errors in numerical modeling needs to be estimated. Although far from reality, this section carries out a series of trial simulations to quantificationally study the effect of the cracks' configuration changing on dynamic crack propagation with simple setting.

3.1. Reference model setting

The reference model is a thin epoxy resin plate with two anti-symmetric notches located in the middle, subjected to uniform longitudinal uni-axial tensile; see Fig. 2. The material is set to be linearly elastic; see Table 1. For brittle material, a time dependent material strength failure criterion, call Tuler Butcher criterion is adopted [14]:

$$\int_0^{\tau_f} \left(\sigma_1 - \sigma_0\right)^{\beta} dt \geq K_f \,, \tag{1}$$

where σ_1 and σ_0 are principle stress (tensile stress in this problem) and a threshold stress, τ_f is fracture duration and K_f is the stress impulse for failure. It is assumed that $\beta = 2$ and $K_f = 10^{-8}$. σ_0 is set to be the static tensile strength, and τ_f is assigned to be the time step used in the time integration.

Table 1. Material properties of epoxy resin

Young's modulus (Mpa)	3300
Poisson's ratio	0.38
Tensile strength (Mpa)	35.0
Epoxy density (kg/m^3)	1180

The displacement boundary condition is applied; the bottom end of the model is fixed, and the top end is pulled up in Z direction. The crack tip is modeled as a notch of the height 0.6 mm, the vertical surface of the notch is discretized by 2 elements, averagely. The average mesh size is 1.0 mm at the top and bottom surfaces of the notch. Due to this discretization, the time increment is set as $\Delta t = 7.5\text{x}10^{-9}$s.

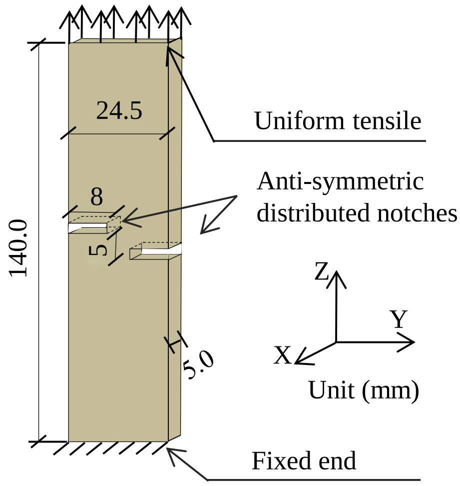

Figure 2. The reference model: epoxy resin thin plate with initial cracks

As aforementioned, the mesh configuration determines the candidate crack paths in PDS-FEM, which introduces local heterogeneity into the target model. In order to reduce the effect of this heterogeneity, finer mesh and lower loading speed can be used. The loading rate is the velocity of the top end, which is set to be V_r = 0.252*m/s*. This velocity is demonstrated to probably generate stable cracks, which means that the crack path solution is not sensitive to the local heterogeneity caused by the mesh setting used in this paper [8]. Also, another mesh with doubled density has been used to make comparison with the current one. The difference is ignorable, which guarantees the availability of current mesh setting for this study.

3.2. Disturbance setting and crack path comparison with reference model

In this sub-section, the near field disturbance is modeled by changing the notches' configuration. The changing is made by adjusting the size, shape and positions of the notches. 3 cases are studied in this part:

(1) Size changing: the left notch size elongates from 8mm to 8.5mm along Y axis, while the right notch size shrinks to 7.5mm.

(2) Position changing: the distance between the anti-symmetric distributed notches changes from 5mm to 4.5 mm.

(3) Out-plane rotation: the notch is designed to rotate along the axis, which is parallel with Y axis, and passes through the centroid of the corresponding notch. Two cases are studied in this paper: (a), left and right notches rotate -5°; and (b), the left rotates -5° and the right rotates 5°. The minus sign indicates that the direction of the rotation points to the Y axis' negative direction according to right hand principle.

(a). Reference model without disturbance

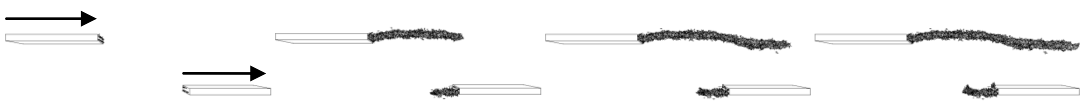

(b). Case 1: left notch elongates 0.5mm, right notches shrinks 0.5mm

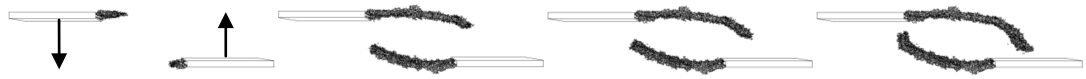

(c). Case 2: the two notches get close to each other by 0.5mm

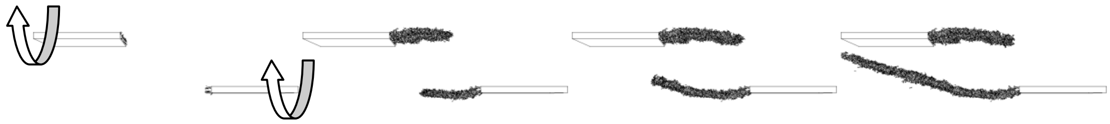

(d). Case 3.a: the two notches rotates 5° in the same direction

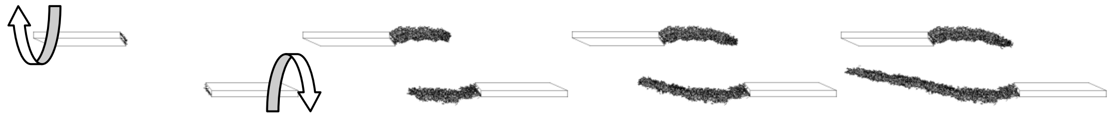

(e). Case 3.b: the two notches rotates 5° in the opposite direction

$t = 30\mu s$ $t = 90\mu s$ $t = 120\mu s$ final state

Figure 3. The near field crack path comparison with reference model

Fig. 3 shows the crack growth process and final states of this dynamic analysis with and without disturbance in notches' configuration. Although the modification is small, the crack path solutions of investigated cases show significant difference except for Case 2. The anti-symmetry property of crack paths solution from the analytical analysis becomes lost [15].

4. Far field disturbance modeling and simulation

4.1. Effect of the degree of heterogeneity

Since the observation technology has its limitation, the boundary condition of analysis model is often proposed in a stochastic way, say, the average with some variances is applied. The variances are used to represent the degree of heterogeneity. The boundary condition with larger variances has stronger effects on crack propagation. The first part of section 4 carries out a series of simulations to numerically examine the effect of the heterogeneity.

The model property is the same as Fig. 2, except that the height is changed to 40mm with the notches still located in the center. In order to avoid element failure near the boundary for the sudden changes caused by the disturbances, the strength of elements within 10mm to the top surface is set to be infinite. The initial tension displacement is 0.075mm for reference model, and the loading rate is set to be uniformly 126mm/s for all the cases. The time step is 5.0×10^{-9} s. Four kinds of disturbance are designed as shown in Table 2. In these formulations, "y" is the Y-axis coordinate of the nodes on top surfaces. The disturbances are added only to the magnitude of nodal displacement boundary condition on top surface along +Z direction. The first one is a half period of sine wave, whose wavelength is 16mm. Case 2 and 3 are two and four periods of sine waves, respectively. The 4th case generates a random number between -0.05mm and 0.05mm for each node on top surface. Except for case 4, the disturbance is set to be uniform along X direction. From Fig. 4, it can be observed that it becomes more and more homogeneous from u_{d1} to u_{d4} (the boundary disturbances are added with 0.075mm in this figure.) For case 4, for a specified area, the average of the disturbance on a certain area tends to be 0. By comparing the stress distribution of models with only these four kinds of disturbance as boundary condition on top surface, u_{d4} leads to weaker effect for far field stress and larger analysis model; see Fig. 5 (a-d).

Table 2. Four kinds of disturbance added to the displacement boundary condition of the nodes on top surface

Case No.	Formulation of disturbance (mm)
1	$u_{d1} = 0.05 \cdot \sin\left(\frac{y+12.25}{8}\pi\right), -12.25 \le y \le -4.25.$
2	$u_{d2} = 0.05 \cdot \sin\left(\frac{y+12.25}{12.25}2\pi\right), -12.25 \le y \le 12.25.$
3	$u_{d3} = 0.05 \cdot \sin\left(\frac{y+12.25}{12.25}4\pi\right), -12.25 \le y \le 12.25.$
4	$u_{d4} = 0.05 \cdot random(-1,1).$

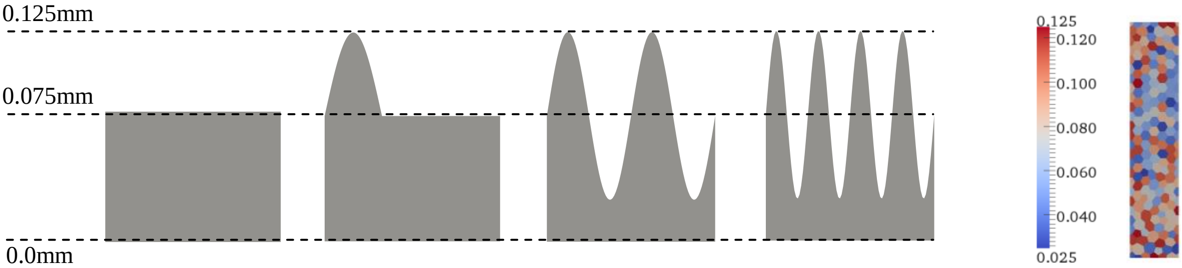

(a) Case 0 (reference) (b) Case 1 (c) Case 2 (d) Case 3 (e) Case 4

Figure 4. Initial displacement boundary condition with disturbances on the top surface (0.075+ $u_{d1\sim}u_{d4}$) mm

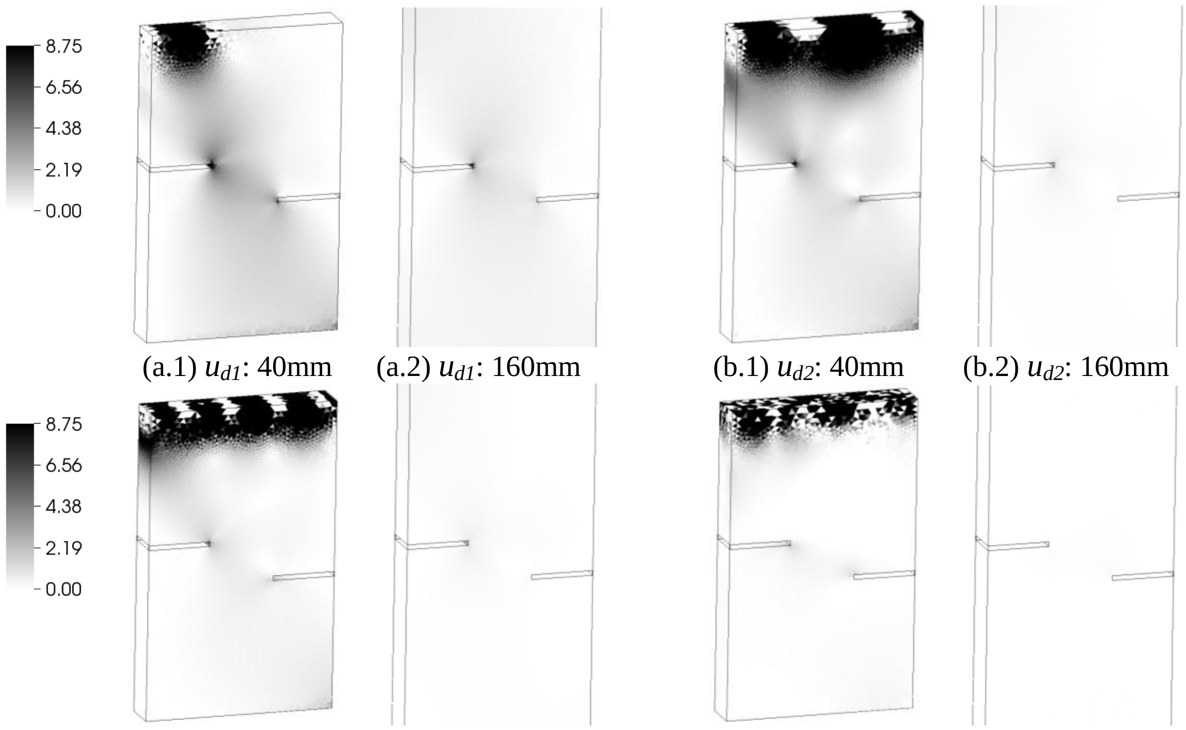

(a.1) u_{d1}: 40mm (a.2) u_{d1}: 160mm (b.1) u_{d2}: 40mm (b.2) u_{d2}: 160mm

(c.1) u_{d3}: 40mm (c.2) u_{d3}: 160mm (d.1) u_{d4}: 40mm (d.2) u_{d4}: 160mm

Figure 5. The tensile principle stress distribution under four kinds of disturbance ($u_{d1\sim}u_{d4}$) with different model sizes (left 40mm height, right 160mm height)

(a). Reference model without disturbance

(b). Case 1

(c). Case 2

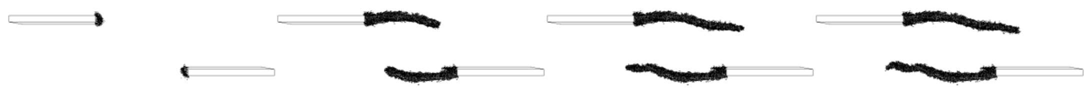

(d). Case 3

(e). Case 4

$t = 0\mu s$ $t = 10\mu s$ $t = 20\mu s$ $t = 100\mu s$

Figure 6. The crack growth process under different boundary condition

Fig. 6 shows the simulation results. From case 1 to case 4, the crack growth process becomes gradually closer to the one of reference model. The most significant difference happens in the case 1, whose average value of boundary displacement on the top surface is the largest. While the smallest difference is observed in case 4, since the disturbance is added node-wisely, the average value tends to be zero in a relative smaller area compared with case 2 and 3, and it is numerically proved here that the disturbance of this kind has smaller effect on the far field crack growth as expected.

4.2. Effect of distance

The Saint-Venant principle tells that if the distance from the area with disturbance increases, the effect will decrease. The accuracy of observation data is constrained to a certain range. This error could be ignored, since the additional strain becomes smaller as the size of analysis model becomes bigger. However, since the crack growth is a non-linear process, numerical estimation is needed to decide the size of analysis model to ignore the disturbances in boundary condition.

This target is similar with the reference model in section 3. The only differences are made in the length in Z direction and boundary condition. The model height becomes 80mm, 160mm and 320mm. As the model size becomes bigger, the distance between the notches and the top surface, where disturbance exists, becomes longer. In order to keep the same strain rate of these models, the boundary condition is defined as Table 3. The disturbance of Table 2- Case 2 is used in this section. All the models of different heights are assigned with the same disturbance.

Table 3. Boundary condition of models with different sizes

Height of the model (mm)	Initial tension displacement (mm)	Loading rate (mm/s)
80	0.15	252
160	0.3	504
320	0.6	1008

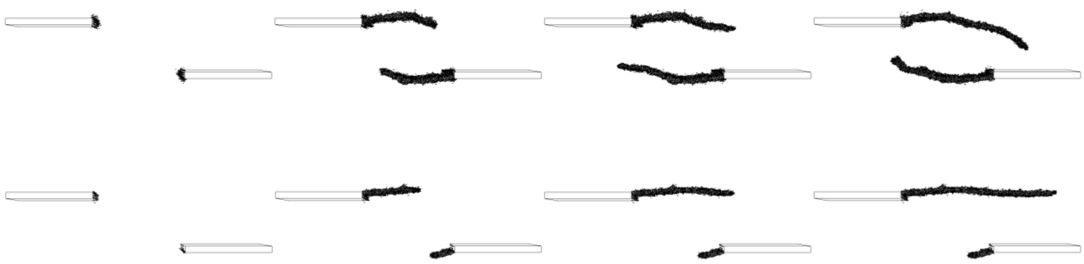

(a). Model of 80mm height without (upper) and with disturbance (lower)

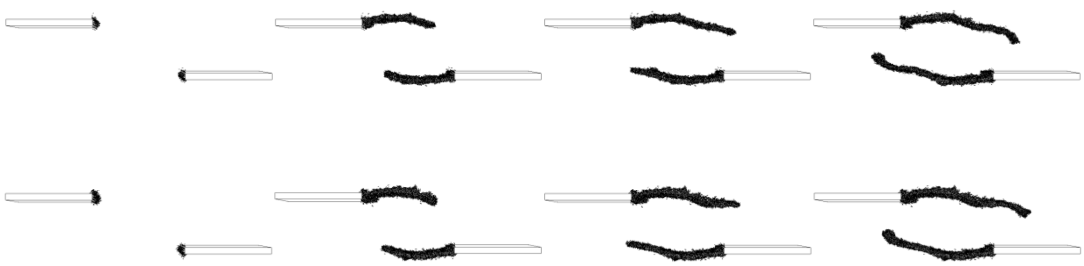

(b). Model of 160mm height without (upper) and with disturbance (lower)

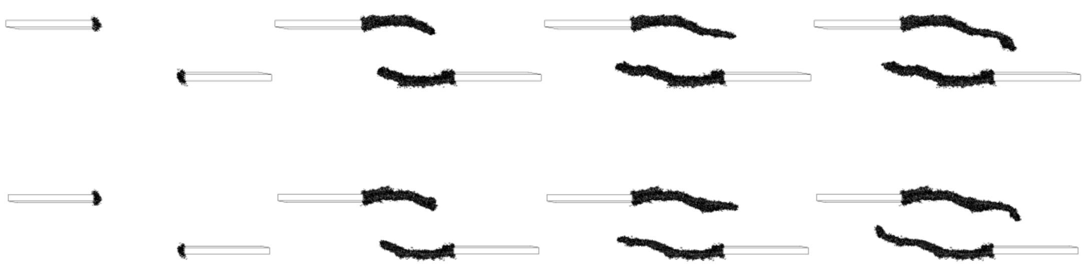

(c). Model of 320mm height without (upper) and with disturbance (lower)

$t = 0\mu s$ $t = 10\mu s$ $t = 20\mu s$ $t = 40\mu s$

Figure 7. The crack path comparison between models with different model height

Fig. 7 shows that the crack path distributions of all the samples without disturbance are anti-symmetric, which are similar to the analytical solution of ideal homogeneous models [14]. Also, these results indicate that the effect of the local heterogeneity generated by these mesh settings can be ignored. As the model size becomes bigger, the difference between models with and without disturbance becomes smaller. For example, the crack path of model of 80mm height with disturbance has one main crack path develop horizontally to the model boundary, the anti-symmetry of crack paths distribution breaks. While, for the models of 160mm and 320mm height, the crack path solutions are almost the same, which indicates that the designed boundary disturbance has ignorable effect on crack growth for these models sizes. The reasons are: (i), with the same boundary disturbance, the bigger the model is, the smaller the additional stress generated; (ii), as the distance from disturbance becomes bigger, the distribution of additional stress becomes more and more uniform; see the stress distribution comparison between different model sizes in Fig. 5.

5. Conclusion

Nowadays, the observation technology still has some distance to be accuracy enough to generate a numerical model fully describing the real world. With limited data, the differences between numerical modelling and reality exist. For crack propagation problem, which is high non-linear, the effect of the differences is numerically examined by using a simple setting in this paper. For a 3D linear elastic dynamic problem, the near field disturbances lead to significant changes to crack path solution in the invested cases. While, the effect of far field disturbance becomes weaker as the distance from crack tips becomes larger, and becomes stronger as the degree of heterogeneity becomes larger. The Saint-Venant principle still holds in the studied crack growth problem.

Acknowledgements

This research is partially supported by the Central Public-interest Scientific Institution Basal Research Fund of China (Grant No. 2011B-05), China postdoctoral Science Foundation, and Natural Science Foundation of Hei Longjiang Province of China (Grant No. LC2012C32). These supports are greatly appreciated.

References

[1] J. Oliver, Modelling strong discontinuities in solid mechanics via strain softening constitutive equations. Part 1: Fundamentals. Int. J. Num. Meth. Eng., **39**(21), (1996) 3575-3600.
[2] K. Ravi-Chandar, and W. Knauss, An experimental investigation into dynamic fracture: III. On steady-state crack propagation and crack branching. International Journal of Fracture, 26(2), (1984) 141-154.
[3] K. Oguni, L. Wijerathne, T. Okinaka and M. Hori, Crack propagation analysis using PDS-FEM and comparison with fracture experiment. Mech. Mater. Phys. Solid, 41(11), (2009) 1242-1252.
[4] J. Oliver, A. Huespe and P. Sanchez, A comparative study on finite elements for capturing strong discontinuities: E-FEM vs X-FEM. Comput. Method Appl. M., 195(37), (2006) 4732-4752.
[5] F. Stan, Discontinuous Galerkin method for interface crack propagation. Int. J. Mater. Forming 1, (2008) 1127-1130.
[6] W.K. Liu, S. Hao, T. Belytschko, S.F. Li, and C.T. Chang, Multiple scale meshfree methods for damage fracture and localization. Comp. Mater. Sci., 16(1), (1999) 197-205.
[7] M. Hori, K. Oguni, and H. Sakaguchi, Proposal of FEM implemented with particle discretization for analysis of failure phenomena. J. Mech. Phys. Solids: 53(3), (2005) 681-703.
[8] H. Chen, L. Wijrathne, M. Hori, and T. Ichimura, Stability analysis of dynamic crack growth using PDS-FEM. Struct. Eng. Earthq. Eng., 29(1), (2012) 1s-8s.
[9] L. Casett, Efficient symplectic algorithms for numerical simulations of Hamiltonian flows. Phys. Scripta, 51, (1995) 29-34.
[10] H. Hausmann, S. Hoyer, B. Schurr et al., New seismic data improve earthquake location in the Vienna basin area, Austria. Austrian Journal of earth sciences, 103(2), (2010) 2-14
[11] J. Tarasewicz, R. S. White, B. Brandsdóttir and B. Thorbjarnardóttir, Location accuracy of earthquake hypocentres beneath Eyjafjallajkull, Iceland, prior to the 2010 eruptions. JKULL, 61, (2011) 33-50

[12] D.R. Shelly, W.L. Ellsworth, T. Ryberg et al., Precise location of San Andreas Fault tremors near Cholame, California using seismometer clusters: Slip on the deep extension of the fault? Geophysical research letters: 36, (2009) L01303, doi:10.1029/2008GL03637
[13] T. Furumura, T. Hayakawa, M. Nakamura, K. Koketsu, and T. Baba, Development of Long-period Ground Motions from the Nankai Trough, Japan, Earthquakes: Observations and Computer Simulation of the 1944 Tonankai (Mw 8.1) and the 2004 SE Off-Kii Peninsula (Mw 7.4) Earthquakes. Pure and Applied Geophysics, (2008)1-23, DOI 10.1007/s00024-008-0318-8.
[14] B.M. Butcher, L.M. Barker, D.E. Munson and C.D. Lundergan. Influence of Stress History on Time-dependant Spall in Metals. AIAA, Vol. 2:6, (1964) 977-990.
[15] A. Sato, Y. Suzuki, D. Fukahori and K. Sugawara, Application of stress compensation-displacement discontinuity method (SC-DDM) to the crack propagation analysis of multi-crack problem. Shigen-to-Sozai, 120, (2004) 493-499. (In Japanese)